Cell, Vol. 83, 693–701, December 1, 1995, Copyright © 1995 by Cell Press

Axon Membrane Flows from the Growth Cone to the Cell Body

Jianwu Dai and Michael P. Sheetz
Department of Cell Biology
Duke University Medical Center
Durham, North Carolina 27710

Summary

During the growth of axons, the surface area of the neuron increases dramatically. Membrane addition as well as exchange could contribute to rapid membrane dynamics or flow. Using diffusing latex beads to monitor membrane flow, we find that axonal membrane flows rapidly (7 μm/min) from growth cone to cell body during axon growth and that flow is inhibited by brefeldin A. To power this flow, there is a membrane tension gradient from growth cone to cell body that could draw the membrane over the axon at that rate. Further, when an artificial flow is induced to the center of the axon by use of laser tweezers, the primary source of the membrane is from the growth cone. We suggest that during neuron growth, there is excess membrane added at the growth cone in chick dorsal root ganglia (DRGs) that undergoes endocytosis at the cell body, thereby creating a flow that can rapidly alter the content of the axon membrane.

Introduction

Nerve growth involves a major increase in the surface area of the cell and requires the constant assembly of surface structures at the growth cone. Because the ribosomes of a developing neuron are mainly confined to the cell body, new proteins are synthesized in the cell body and carried outward in vesicles by anterograde axonal fast transport to the growth cone. Recently, newly synthesized membrane proteins were shown to be preferentially added at axonal growth cones (Craig et al., 1995). A robust endocytosis also occurs at the growth cone, which, when coupled with retrograde fast axonal transport, carries signals back to the cell body. This retrograde traffic could balance the exocytosis of new components. Thus, it is not clear whether the bulk of the axon plasma membrane is added at the cell body or at the growth cone. Contradictory results were found in previous studies that tried to localize sites of bulk membrane addition in growing neurons (Bray, 1970; Griffin et al., 1981; Pfenninger and Maylie-Pfenninger, 1981; Popov et al., 1993; Craig et al., 1995). If axon membrane movement during neurite extension can be measured, the balance of membrane trafficking, the site of bulk membrane addition, and the rate axon membrane exchange can be defined.

Because there is evidence for both secretion and endocytosis at the growth cone, other experiments are needed to determine whether the axon membrane is stationary or flows in an anterograde or retrograde direction. The direct analysis of membrane movement has been difficult, and most arguments have been indirect. A direct approach for probing net flow in the plasma membrane plane is the single particle tracking (SPT) technique, in which membrane proteins or lipids are tagged with antibody–coated submicrometer colloidal gold or latex particles, and the trajectories of the labeled molecules are followed by observing the particle movement (Lee et al., 1991; Kucik et al., 1990; Sheetz et al., 1989). The SPT method provides more detailed information about membrane molecule mobility than the fluorescence photobleaching and recovery technique (Qian et al., 1991; Ishihara and Jacobson, 1993), and the technique has been utilized to show that there is no bulk flow of membrane on the surface of migrating fibroblasts (Lee et al., 1993; Kucik et al., 1990; Sheetz et al., 1989). Within neurons, the high degree of asymmetry of the neuritic processes may lead to a flow.

For membrane to flow from one end of an axon to another, there must be a driving force to pull the membrane tube over the axon cytoskeleton. In physical terms, this force must be applied to the axon membrane and would appear as a tension in the plane of that membrane. Because of the fluid nature of plasma membranes, a tension in the membrane plane is isotropic. If the membrane is deformed, then the tension will produce a restoring force, and the magnitude of the restoring force can be used to estimate the membrane tension. In practice, when membranes are deformed, a thin membrane tube or tether is produced, and the membrane tension creates a restoring force on that tether (Waugh and Hochmuth, 1987). We can readily measure the restoring force on membrane tethers with the laser tweezers, thereby giving a direct estimate of that tension (Dai and Sheetz, 1995a). Thus, another way to test whether there is a membrane flow along an axon is to measure the membrane tension or tether force at different regions along the axon surface. If there is a membrane flow, the tension should be smaller at the origin of the flow, because there is excess membrane in that region.

Another way to probe where axonal membranes come from is to remove membrane from the center of the axon and ask whether the replacement membrane is drawn from the cell body or the growth cone. Because membranes are very inelastic, the movement of membrane into a tether formed on an axon will create a flow of membrane to that site from the preferred site of membrane addition. In previous studies, we have found that membrane can be drawn into tethers from growth cones at rates several hundredfold greater than the natural rate of axon growth (Dai and Sheetz, 1995a). Tether formation can thus be used as a membrane sink to determine where membrane is being added to the axon.

We have used these different criteria to analyze chick dorsal root ganglion (DRG) axons for membrane flow. The results all indicate that there is a membrane flow along the axon from the growth cone to the cell body and that

it can rapidly exchange the contents of the plasma membrane.

Results

Flow of Diffusing Beads

To determine whether the membrane on axons was flowing either to or from the growth cone, we followed the movements of diffusing beads on the axons of chick DRGs. In previous studies, we found that rat immunoglobulin G (IgG)-coated beads would bind to and diffuse on most plasma membranes, including DRG axons. The bound beads did not alter cell motile behavior and continued to diffuse for relatively long periods before binding irreversibly to the glass substrate or the cell cytoskeleton. In quantitative terms, we found that 60% of the rat IgG beads bound to the membranes of chick DRG axons after they were held there for 3 s with the laser tweezers. The majority of the bound beads diffused randomly after release, but approximately 30% of the beads placed on the axons did not diffuse randomly, suggesting that some rigid contacts with the cytoskeleton were present. The diffusing beads appeared to diffuse rapidly, and when the mean squared displacement (MSD) with time plot of bead movement was analyzed (see Experimental Procedures), an apparent diffusion coefficient of 8.7 ($\pm$ 0.44) $\times$ 10^{-10} cm^2/s (n = 17) was determined, which is typical for membrane glycoproteins in neurons (Sheetz et al., 1990). When diffusing beads were followed over time, they underwent a net displacement toward the cell body (see Figure 1). This was seen most dramatically in the coordinate displacements of several diffusing beads on the same axon. In Figure 1 are three examples of multiple beads bound to the same stretch of axon over a 2–4 min period. The beads diffuse randomly with respect to one another but always undergo a net displacement toward the cell body. Upon tracking the movements of two individual IgG-coated beads on the axon, we find that the X–Y plots of bead position show that the beads sample much of the surface of the axon laterally covering the width of the axon (about 1.4 μm) and the bead diameter of 0.5 μm (see Figure 2A). The axial movements of the beads show diffusive movement as a noise upon which is superimposed movement toward the cell body. Movement is not continuous but shows stationary periods interspersed with periods of movement away from the growth cone, where the slope of the diffusion envelope gives a velocity of 6–8 μm/min. In the same axons, retrograde transport vesicles move at about 240 μm/min and show little diffusion during movement. For two beads on the same axon, the slow and rapid periods of movement are not coordinated, indicating that fluctuations in flow rate are not responsible for the apparent fluctuations in velocity. We measured the net displacements of the beads over a 40–90 s period and obtained an average velocity of 3.61 ($\pm$ 0.43 standard error) μm/min (n = 35). To determine whether there was a significant loss or addition of membrane along the axon, we measured the average flow velocity at the growth cone (V_{GC}) and cell body (V_{CB}) ends of the axon sequentially. No difference in the average flow velocity was found across the axon (the ratio of V_{CB} to V_{GC} was ~0.95, n = 11). The average DRG axon elongation rate was 1.13 $\pm$ 0.19 μm/min (n = 28) in the same preparation. When the axons were incubated at 29°–30°C, which blocked elongation, the average velocity of flow dropped to 1.17 $\pm$ 0.22 μm/min (n = 8). Thus, the rat IgG beads do undergo a regular displacement toward the cell body, consistent with diffusion on a membrane flowing from the growth cone to the cell body.

Flow of Lipid-Attached Beads

It is possible that the rat IgG is bound to an unusual glycoprotein that is moved to the cell body; therefore, we examined the behavior of beads linked to membrane lipids. Beads (0.5 μm in diameter) were coated with an anti-fluorescein monoclonal antibody and were bound to axons labeled with fluorescein-modified phosphatidylethanolamine (FL-PE) (Lee et al., 1991). When the beads were held by laser tweezers for 3 s on axon membranes containing FL-PE, 18% of the beads were bound and diffused on the axon surface after the tweezers was turned off. Binding dropped to 2% when free fluorescein (2 μg/ml) was added and to 1% when no FL-PE was added to the membranes. Bound beads diffused randomly along the axon with an apparent diffusion coefficient of 2.41 ($\pm$ 0.68) $\times$ 10^{-9} cm^2/s (n = 23). It was noted that the diffusing beads normally were biased in their diffusion toward the cell body. Figure 2B shows that the beads sampled much of the surface of the axon, and the axial movements show a wider diffusion envelope and a steadier movement toward the cell body than the IgG beads, at an average velocity of 6–9 μm/min. When the displacements were recorded over a 40–90 s period and expressed as a velocity, an average apparent velocity of 6.87 (standard error, $\pm$0.79) μm/min (n = 33) for anti-fluorescein-bound beads was obtained, which was significantly different from the velocity for IgG beads ($P < 0.001$). Doping of the membranes with FL-PE did not significantly alter the average elongation rate of the axons (1.06 $\pm$ 0.14 μm/min [n = 17]). The anti-FL antibody–coated latex beads diffused faster than the IgG beads and

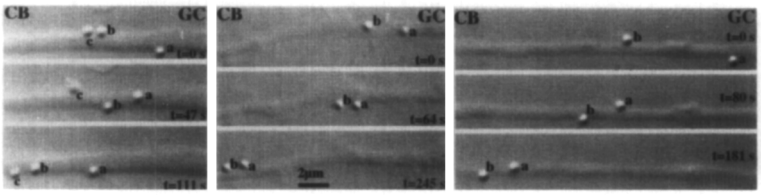

Figure 1. Photomicrographs of Three Examples of Multiple Beads Bound to the Same Stretch of Axon over a Period of Two to Four Minutes

These diffusing beads walk randomly with respect to one another but always undergo a net displacement toward the cell body. The times are noted, and the beads are identified.

moved toward the cell body at a higher average rate. The average diameter of the axons was 1.38 ± 0.32 (n = 48) μm, as determined by analyzing the video images; consequently, we estimate that an area of approximately 30 μm^2 of membrane is moving rearward per minute.

Another way to analyze the motion of the beads is illustrated in Figure 3, where the diffusive and flow components of beads are separated mathematically in a modification of the diffusion equation. An MSD versus time plot for a diffusing bead on a flowing membrane will have a quadratic term that represents the flow. For anti-FL antibody beads, we find an upward curvature of the MSD versus time plots, indicating that the movement of the beads includes both directed and diffusive motion (Figure 3). Using the equation $MSD = 2Dt + (vt)^2$, we find that the average velocity (v) of the directed movement of the bead from the growth cone to the cell body in this case is 11.7 μm/min, which is similar to the velocities that were calculated from net displacements of the beads that diffused for 40–90 s. Mathematical analysis of the lipid bead diffusion also provides evidence of a rapid flow in addition to diffusion.

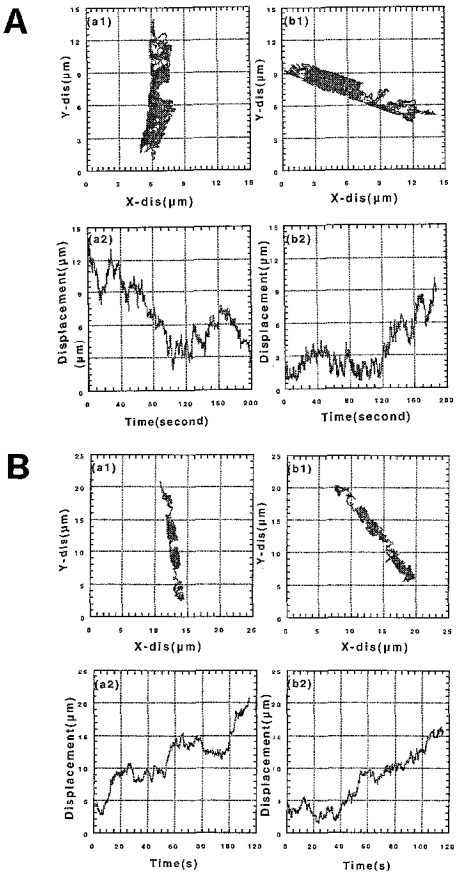

Figure 2. Plots of IgG and Anti-FL Antibody Beads

(A) Plots of IgG bead positions, either X–Y (a1 and b1) or parallel displacement with time (a2 and b2) of two diffusing beads over a 200 s period. X–Y plots (a1 and b1) show that the beads (0.5 μm in diameter) sample the whole surface of the axons (average 1.4 μm in diameter). Parallel displacement with time plots (a2 and b2) show diffusive movement, and at times a directed movement toward the cell body is superimposed.

(B) Plots of anti-FL antibody bead positions, either X–Y (a1 and b1) or parallel displacement with time (a2 and b2) of two diffusing beads over a 120 s period. X–Y plots (a1 and b1) show that the beads (0.5 μm in diameter) sample the whole surface of the axons (average 1.4 μm in diameter). Parallel displacement with time plots (a2 and b2) show diffusive movement with a directed movement toward the cell body superimposed. The overall rate of movement (about 7 μm/min) is similar to the maximum rate of movement of the IgG beads.

Tether Force Is Greater at the Cell Body End of the Axon

For the membrane to flow from the growth cone to the cell body, there must be a force pulling or pushing it over the axon cytoskeleton. From previous studies, it is clear that the plasma membranes of most cells, including neurons, are drawn down onto the cytoskeleton through adhesion to the cytoskeleton and a membrane tension that would stretch the membrane. This suggests that the membrane would be pulled toward the cell body by a greater membrane tension at the cell body. Further, the fluid nature of membranes would not support a pushing force. A membrane tension is isotropic and will resist deformation of the membrane in all directions. We can deform axon mem-

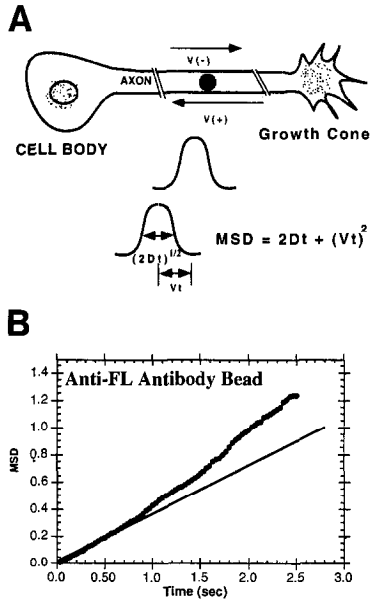

Figure 3. Illustration of the Mathematical Description of Diffusion on a Flowing Membrane and Actual Analysis of Anti-FL Antibody Bead on an Axon

(A) shows the mathematical description of diffusion on a flowing membrane; (B) is the actual analysis of an anti-FL antibody bead on an axon.

The diagram (A) shows that if the bead was diffusing as the axon membrane was moving, then the normal diffusion envelope was simply displaced by the product of the velocity and the time. The MSD of the beads can be described by the following equation: $MSD = 2Dt + (vt)^2$ (Sheetz et al., 1989), where D is the apparent diffusion coefficient, t is the time interval, and v is the velocity of the flow.

In (B), an MSD versus time plot of an anti-FL bead moving on an axon (dotted line) shows a positive deviation from linearity. The curve is best fit with a quadratic equation including terms for diffusive movement (straight line, with an apparent $D = 2.3 \times 10^{-9}$ cm^2/s) and flow at an average velocity of 11.7 μm/min.

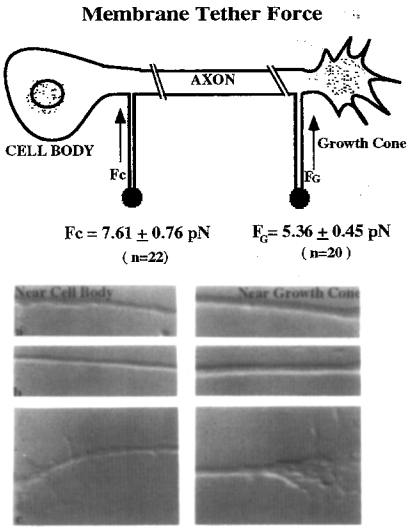

Figure 4. Tether Force Is Greater and Axon Diameter Is Smaller at the Cell Body Than at the Growth Cone

The diagram shows that the static tether force near the cell body is significantly greater ($P < 0.02$) than the force at the growth cone. The photomicrographs show that the axon diameter is significantly smaller near the cell body than near the growth cone (the ratio of diameters at the growth cone to those at the cell body is 1.57 ± 0.07 [standard error, n = 21]).

branes in a controlled way with a laser tweezers force applied to the membrane-attached beads. Pulling on the beads will produce a thin membrane tube or tether (see Figure 4), and the force on that tether can be related to the membrane tension (Hochmuth et al., 1995). There are several terms in the tether force, including the membrane bending stiffness, the membrane adhesion to the cytoskeleton, and a mechanical in-plane tension. Because there is no way to separate the membrane adhesion from the in-plane tension terms for a cell that has a complex shape, such as a neuron, we have included both terms in what we are defining here as a membrane tension (Dai and Sheetz, 1995b; Hochmuth et al., 1995). Thus, for a membrane flow from the growth cone to the cell body, there must be a driving force of a higher membrane tension at the cell body.

To explore whether a membrane tension could drive this flow, tethers were formed on axons either 4 μm from the cell body or 4 μm from the growth cone. The force exerted by the tether on the bead was determined from the displacement of the bead from the center of the tweezers (Dai and Sheetz, 1995a). Tethers were 10 μm in length and were held stationary for 10–20 s. As in previous studies, the force on the bead was independent of tether length in the range of 5–30 μm (Dai and Sheetz, 1995a). The axons were 60–100 μm in length. Figure 4 shows that the force exerted by the tether was on average 2.25 pN greater at the cell body than at the growth cone ($P < 0.02$). In addition to the membrane tension, the membrane bending stiffness contributes to the force on a tether (Hochmuth et al., 1995). If the membrane bending stiffness was the same at both ends of the axon, the diameter of the tether should be inversely related to the tether force. When we measured the apparent diameters of the tethers at the cell body and the growth cone from the relative contrast of the tethers (Schnapp et al., 1988), we found that the tethers at the growth cone were 1.24-fold ± 0.10-fold (n = 21) larger than those at the cell body. This is within experimental error of the inverse ratio of tether forces (1.38 ± 0.14, n = 20). Thus, we find that the membrane tension is greater at the cell body than at the growth cone and would drive membrane movement in that direction.

The greater membrane tension at the cell body would produce a compressive pressure on the axon, which may result in the constriction of the axon at the cell body. When the axon diameters were compared for points 4 μm from the cell body versus 4 μm from the growth cone, the axon at the growth cone was 1.57-fold ± 0.07-fold (n = 21) larger than at the cell body. This dramatic difference in diameter is seen in stretches of the axon that are clearly separated from the growth cone (Figure 4) and show no tapering. A thinning of the axon near the cell body is observed, which is consistent with the higher membrane tension observed there.

A test of whether tension does drive the flow is to determine the rate of membrane flow supported by the observed tension difference. In other words, a flow velocity can be calculated from the viscous resistance of the axon and the tension difference, which should correspond to the velocity observed by the bead movements. The viscous resistance of the axon was derived from the changes in tether force with changes in velocity of tether formation, which were shown previously to be linearly related (Dai and Sheetz, 1995a). We found that the force on the tether increased 1.5 pN per μm/s increase in the velocity of tether extension for tethers formed in the center of the axon. As a test of the linearity of the tension along the axon, we measured the tether force at zero velocity to be 6.08 pN, which is indeed intermediate between the tether forces at the cell body and growth cone. The average tether diameter was estimated from the relative contrast of the tether to be about 0.4 μm (1.26 μm^2 of membrane per micrometer of tether). Thus, we estimate that 56 μm^2 of membrane per minute would be moved by a gradient in tension corresponding to a difference of 2.25 pN in the tether force over the length of the axon (Figure 4). This is in excess of the observed value of 30 μm^2/min for the lipid-attached beads. Thus, the membrane tension difference between the cell body and the growth cone is sufficient to account for the observed membrane flow.

Tether Formation and Membrane Flow

Another way to test whether membrane is being preferentially added to the axon at the growth cone is to create a membrane flow in the center of the axon by forming a membrane tether with the laser tweezers. We formed membrane tethers with an apparent diameter of 0.4 μm that were extended rapidly to a length of 15–20 μm (velocity was 5–10 μm/s). This created a flow of 19–25 μm^2 of membrane to the site of tether formation. Diffusing beads on the axon should flow toward the tether site from the site of membrane addition to the axon. Two diffusing beads were placed on an axon, one on either the cell body or

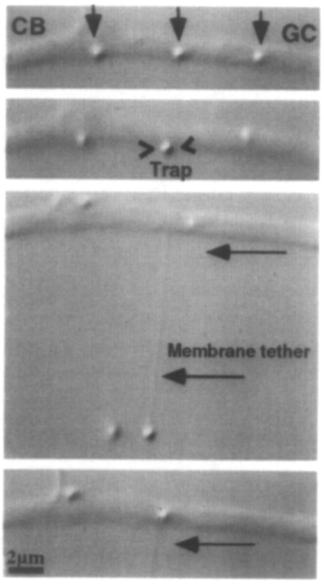

Figure 5. Photomicrographs Show That the Membrane Flows Primarily from the Growth Cone to the Tether Site

In the first panel, three diffusing IgG beads are shown on the axon. In the second panel, the central bead is trapped by the laser tweezers. Then a tether of 15 μm is formed at a rate of 5 μm/s with the central bead, and there is obvious movement of the bead on the growth cone (GC) side but not the cell body (CB) side of the tether. The final panel shows an in focus view of the beads on the axon.

the growth cone side of the tether. After a tether was pulled, the bead on the growth cone side of the tether moved toward the tether site, whereas there was barely detectable movement of the bead on the cell body side (Figure 5). On average, the anti-FL bead displacements were 0.89 ± 0.25 μm (standard error, n = 20) and 4.12 ± 0.28 μm (standard error, n = 29) for the beads on the cell body and growth cone sides, respectively (Figure 6A). Similarly, with the IgG beads, the displacements on the cell body and growth cone sides were 0.74 ± 0.15 (standard error, n = 52) and 4.15 ± 0.40 (standard error, n = 87) μm, respectively (Figure 6B). Because the flow onto the tether was rapid, the sum of the net particle displacements corresponded to the amount of axonal membrane moved into the tether, or on average, 22 μm^2. Thus, about 80% of the membrane that was drawn into a tether came from the growth cone, while only 20% from the cell body (Figure 7).

Flow from the Growth Cone Is Inhibited by Brefeldin A

If the flow of membrane from the growth cone results from the incorporation of membrane into the growth cone through a normal secretion process, then the addition of brefeldin A, which partially inhibits transport in axons (Smith et al., 1994), should cause a decrease in the flow. Cells were treated with 5 μg/ml of brefeldin A for 1 hr prior to analysis. The results showed that for diffusing IgG beads on the axon, the average flow velocity was 3.61 ± 0.43 μm/min (n = 35) but was reduced to 1.55 ± 0.45 μm/min (n = 14) when cells were treated with brefeldin

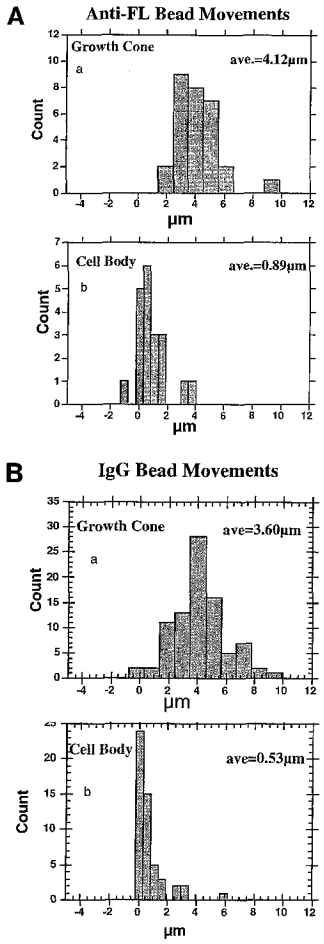

Figure 6. Quantitation of Tether-Induced Flow

These histogram plots show the distance that anti-FL (A) or IgG (B) beads moved toward the tether when the diffusing beads were on either the growth cone (A) or the cell body (B) side of the tether. Tethers of 15–20 μm in length were formed at a rate of 4–10 μm/s. There are no significant differences between the average displacements of anti-FL- versus IgG-coated beads.

A. There was a 2-fold decrease ($P < 0.05$) in the apparent flow rate of beads coated with rat IgG in the presence of brefeldin A.

Discussion

All of these findings suggest that there is a net flow of plasma membrane from the growth cone to the cell body. Diffusing beads on the axon flow from the growth cone to the cell body, and a membrane tension gradient exists that would drive the membrane in that direction. Further, induction of a flow of membrane into an axon tether draws membrane primarily from the growth cone. We estimate that the flow rate is in excess of 7 μm/min, on the basis of the lipid-attached bead transport rate and the tension drop across the axon. From the rates of flow observed, the whole membrane of an axon 200 μm in length could be exchanged in 30 min or less.

Several alternative hypotheses can be readily ruled out.

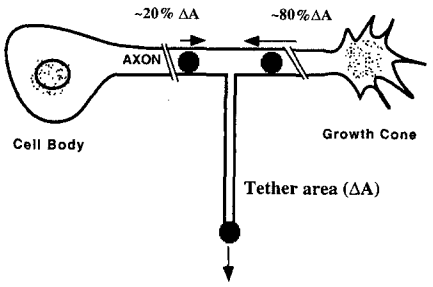

Figure 7. Summary Diagram for the Induced Membrane Flow Experiments

The diagram shows that 80% of the tether membrane comes from the growth cone side, and 20% comes from the cell body side. The area of membrane estimated to be in the tether equals that calculated from the movement of the beads on the axon.

Active retrograde cytoskeletal transport could cause rearward surface particle movement on axons by a mechanism similar to the forward movements of particles on growth cones (Sheetz et al., 1990). Such transport could not explain either the rapid flow of membrane from the growth cone to the tether site when flow is induced or the greater membrane tension at the cell body end of the axon. In another scenario, both the greater membrane tension at the cell body end of the axon and the decreased flow from the cell body could result from a stronger attachment of membrane to the cytoskeleton at the cell body. However, that would not explain the flow of diffusing beads. The simplest explanation for all three types of observations is a rapid flow of membrane from the growth cone to the cell body.

In the diffusing bead measurements, the velocity of flow of the two sets of beads differed by approximately a factor of two, as did the diffusion coefficients. The more rapidly diffusing beads were displaced further. This could be explained by suggesting either that the slower diffusing IgG beads were interacting selectively with the cytoskeleton, or that there was a direct correlation between the diffusion coefficient and flow rate. If the second case were true, there would be a dramatic concentration of proteins in the axon because of their slower diffusion and consequently slower transport rate. There is synthesis of lipid in the distal portions of growing axons (Vance et al., 1991) that could serve to dilute the membrane proteins in the anterogradely transported vesicles. In that case, the difference in flow rates would serve to reconcentrate proteins in the axon plasma membrane. Alternatively, the IgG beads interact much more strongly with the cytoskeleton than uncross-linked proteins, slowing their flow significantly. In this case, the flow rate of the lipid-linked beads would represent that of the bulk membrane, and concentration would only occur upon selective binding to the cytoskeleton. Since the IgG beads often experience periods where they are not flowing, they do appear to be held back by barriers to diffusion. In previous studies of bead movement on axons, larger beads were used, which were attached to the cytoskeleton (evidenced by the lack of bead diffusion), and no retrograde movement was observed (Bray, 1970; Popov et al., 1993). In the chick DRG axon, the bulk of the cytoskeleton appears stationary (Martenson et al., 1993; Okabe and Hirokawa, 1993), and a greater interaction of the IgG beads with the cytoskeleton could dramatically reduce the apparent velocity. Further analysis is needed to differentiate between a diffusion-related mechanism for slowing the IgG bead movement and a selective interaction with the cytoskeleton. If the correlation between diffusion coefficient and flow can be extrapolated for the free lipids, then the free lipid flow rate may be even greater than the value observed here. Consequently, we suggest that the actual flow rate is equal to or greater than the observed 6.7 μm/min.

Because of the large size of the beads, 0.5 μm, with an estimated membrane contact area of 0.2–0.3 μm in diameter, even the lipid-bound beads will be in contact with some membrane proteins. It is perhaps surprising that the beads are not bound to the cytoskeleton. However, in other systems, the distance between rigid barriers to diffusion is on the order of one to several micrometers (Debrabander et al., 1991; Edidin et al., 1991; Sheetz et al., 1989). The cross-linking of lipids by particles slows their apparent diffusion coefficient by nearly 2-fold in other systems (Lee et al., 1993), and the observed diffusion coefficients for the FL-PE attached beads are very similar to those earlier measurements. Further, the diffusion coefficient of the IgG beads was similar to that observed for specific antibodies to neuronal proteins (Sheetz et al., 1990). The quantitative characteristics of the bead diffusion are in line with previous observations.

For the membrane to flow, there must be a force driving it. When we measured the force on static tethers at the cell body and growth cone ends of the axon, we found a 2.25 pN difference in the tether force that was due to a difference in membrane tension. Because the velocity of tether formation was linearly related to the force on the tether (Dai and Sheetz, 1995a), we could estimate the velocity of flow supported by that tension difference. Assuming that the drag from the center of these axons (1.5 pN/μm/s) was half the drag of the whole axon and that the diameters of the tether and axon were 0.4 and 1.38 μm, respectively, we calculated that a flow rate of 57 μm^2/min would be driven by the tension corresponding to a 2.25 pN force drop. These results further support the possibility that the actual flow rate is greater than observed.

In other studies, we have found that membrane tension is a highly regulated parameter and have proposed that it can be used to control membrane surface area (Dai and Sheetz, 1995b). The forces generated by membrane tension are sufficient to inhibit molecular motors mechanically (Svoboda et al., 1993; Kuo and Sheetz, 1993). Previous findings showed that the laser tweezers ligation of vesicle transport in chick DRG axons blocked axon elongation (Martenson et al., 1993). A consequence of the block of membrane addition at the growth cone would be a rise in the membrane tension that could logically inhibit extension of filopodia and would favor retraction of the growth cone. In the case of axonal flow, the membrane tension provides a driving force for the membrane flow. In addition, the greater tension at the cell body end of the axon would produce a greater constricting force on the axon that could

produce the smaller diameter of the axon at that end. Because membrane tension is propagated through the membrane, alterations in membrane tension can have general effects on cell functions such as endocytosis rate or motility. Having a source of membrane at the growth cone would naturally decrease the membrane tension in that region and would favor extension and motility.

When a flow of membrane was induced by tether formation, the source of membrane was primarily the growth cone for both the anti-FL and IgG beads. The fraction of membrane added from the cell body was low and was consistent with the high force used to form the tether at a rapid rate, since that force exceeded the force of stationary tethers at the cell body end of the axon. There was a balance of the membrane area in the tether with the area lost from the axon. The calculated area of the tether matched the calculated area of axon membrane lost for both types of beads; therefore, we suggest that the membrane in the tether was representative of the membrane in the axon. If only a fraction of the axon lipids or proteins were allowed onto the tether, then the area of the tether could be significantly greater than the area estimated from the axonal bead movements. Tethers were very fluid, and they behaved as other tethers in which the barriers to diffusion had been stripped away (Berk and Hochmuth, 1992). These findings are consistent with the suggestion that the tether samples the majority of the membrane and that only a small fraction of the membrane is attached to the cytoskeleton such that it is prevented from entering the tether. For the induced membrane flow, both IgG beads and lipid-bound beads showed equal displacements, whereas displacements of lipid-bound beads were 2-fold greater during normal axon flow. The reason for this might be that there are very different rates of flow in the two experiments. The induced flow is very fast, and diffusion can be neglected. But for the normal flow, slower diffusion and trapping may explain the slower rate of movement of the IgG beads. In fact, there are often stationary periods during the direct movement of IgG beads, while the lipid-bound beads move almost continuously.

For the membrane flow to continue, there must be a replenishment of the membrane at the growth cone through internal, anterograde transport. The addition of brefeldin A to DRG neurons in the frog was shown to inhibit the anterograde axonal transport partially (Smith et al., 1994). Brefeldin A caused a 2-fold decrease in the rate of flow of IgG beads, consistent with the partial inhibition of axonal transport. Measurements of spherical vesicle transport have not shown a dramatic excess in the anterograde movements that could account for the flow observed. Alternatively, the tubular vesicular membranes of the smooth endoplasmic reticulum could provide a source of the membrane. Thus, the flow is dependent on secretory membrane traffic, but the nature of the vesicles is unknown. Membrane addition or subtraction along the axon could dramatically alter the rate of flow at the two axon ends, but we observe essentially the same flow rate at the growth cone and the cell body. Because of the constriction of the axon at the cell body end, there may be as much as one third of the axon membrane taken in along the axon. From these findings, it is clear that membrane is flowing the full length of the axon at approximately the same velocity.

The flow of membrane from the growth cone to the cell body in chick DRG axons is quite high. The measured flow rates are considerably greater than the elongation rate of the axon (1.13 ± 0.19 μm/min, n = 28). These findings are consistent with the earlier observations (Pfenninger and Maylie-Pfenninger, 1981) of clearance of bound lectins from the growth cones and migration toward the cell body. The lectins could perturb the glycoproteins, but the basic interpretation was that the membrane was flowing in a retrograde direction on rat superior cervical ganglia axons. In the frog axons, flow was observed in the opposite direction by the movement of incorporated lipid dye and by beads that were attached to the axon cytoskeleton (evidenced by the fact that they were not diffusing) (Popov et al., 1993). In studies of the axon microtubules, dramatic differences were also seen between frog and rat DRG systems; they are consistent with the differences seen here (Reinsch et al., 1991; Okabe and Hirokawa, 1990, 1993). Namely, telescoping of the microtubules in the axons of the frog was observed, which could account for the forward movement of membrane as well. In the rat DRGs, no microtubule movements were seen, indicating fundamental differences in the extension processes between the two systems. In other rat axon studies, there is evidence for the preferential insertion of newly synthesized membrane proteins at the growth cone and their subsequent movement over the whole axon (Craig et al., 1995). All of these studies do indicate that the rapid process extension of frog neurites differs from the extension of avian or mammalian DRG axons and that the assembly of structures at the growth cone is greater in those systems, which is consistent with the flow from the growth cone to the cell body.

Membrane flow over the axon can have several functions, but others can be ruled out. First, we can say that membrane addition is not the rate-limiting step in axon elongation. Axon membrane flow is nearly 5-fold greater than the elongation rate, and the movement of membrane onto tethers at rates over 100-fold greater than the elongation rate requires tensions considerably smaller than those generated by growth cones (Heidemann et al., 1990). Secondly, flow was suggested as an important driving force for cell migration (Bretscher, 1984); however, many studies showed that a bulk flow of membrane does not occur in migrating cells (Sheetz et al., 1989; Kucik et al., 1990; Lee et al., 1990). In this case, the force that could be generated on a stationary membrane contact would be very small, as estimated from the rapid diffusion of even 0.5 μm spheres on the axon. Plus, the tension produced would be several orders of magnitude too low to account for the forces that growth cones normally develop on matrix contacts (Heidemann et al., 1990). Rather, we speculate that the membrane flow serves to replenish the components of the axon plasma membrane. Axon membrane needs to be replenished as other membranes (Steinman et al., 1983), except that the exocytosis and endocytosis machinery may complicate the transport process. Instead of a

local exchange of membrane components, a flow could achieve the same end and would avoid the need for membrane recycling machinery in the axon as well as some of the signaling events associated with membrane recycling. In addition, the growing axon will want to change its membrane composition in response to environmental signals that are sensed at the growth cone, and the flow from the growth cone would provide a rapid means of doing so. More analysis of the flow of membrane in synapsed as well as growing axons is needed to understand the biological functions of the axon membrane flow.

Experimental Procedures

Chick DRG Culture

Chick DRG explants were dissected from 12-day-old chick embryos and plated in growth wells on treated coverslips. To prepare the cell growth wells, 20 × 20 mm (number 1) glass coverslips (Becton Dickinson Labware, Lincoln Park, NJ) and 10 mm diameter cloning cylinders (Bellco, Vineland, NJ) were cleaned by soaking in 20% nitric acid for 2–3 hr, followed by rinsing in distilled water for 1 hr. Then they were put into 95% ethanol overnight and rinsed in distilled water for at least 2 hr. After drying and sterilization, a cloning cylinder was secured to the coverslip with sterilized silicone grease to form a growth well. The growth well was coated with 0.01% poly-L-lysine for 15 min at room temperature, rinsed three times with sterilized water, then dried in a sterile hood. Just before the dissection, poly-L-lysine-coated growth wells were exposed to a solution of Matrigel (Collaborative Research, Bedford, MA) and minimal essential medium (MEM) in a 1:50 ratio. Explants were maintained at 37°C, 5% CO_2 in clear MEM (GIBCO BRL, Grand Island, NY) supplemented with the following: 20 mM HEPES, 6 mg/ml glucose, 5 μl/ml penicillin/streptomycin (GIBCO), 2 mM L-glutamine, 10 μl/ml N2 serum-free supplement (GIBCO), and 10 nM/ml nerve growth factor (NGF 2.5s; GIBCO). The explants were used after they had been incubated for 24–48 hr.

Bead Preparation

In previous studies, we observed that covaspheres coated with a control IgG preparation would bind to growth cone membranes without any apparent perturbation of growth cone behavior. To prepare IgG-coated beads, rat IgG (Sigma, St. Louis, MO) was solubilized at a concentration of 10 mg/ml in PBS. Then, 50 μl of covaspheres (0.5 μm, Duke Scientific, Palo Alto, CA) was added to 50 μl of the above IgG solution and was incubated at 4°C overnight. The beads were pelleted by centrifugation at 2000 × g and 4°C for 10 min. Then the beads were resuspended in 1 mg/ml BSA–PBS solution, rinsed by pelleting and resuspension with MEM three times, and resuspended in 100 μl of MEM. For the experiments, the bead solution was diluted 3:100 in DRG medium. To prepare the anti-FL monoclonal antibody-coated beads, 20 μl of covaspheres was added to 30 μl of 2 mg/ml antibody (Molecular Probes, Eugene, OR) PBS solution. The washing steps were the same as for the preparation of the IgG-coated latex beads.

Calibration of the Laser Tweezers

The laser optical trap was calibrated by viscous drag through the aqueous medium in the microscope focal plane. The viscous force was generated by oscillatory motion of the specimen by a piezoceramic-driven stage (Wye Creek Instruments, Frederick, MD) at a constant velocity. The position of the bead in the trap was tracked by using the nanometer-level tracking program (Gelles et al., 1988) to analyze video records of the experiments. Positional variation of the particle in the trap with 60 mW of laser power entering the microscope was 11 (± 1.7) nm. The calibration showed a very linear force–distance relationship for the optical tweezers. To study the variation in trap calibration with height above the coverslip surface, latex beads (0.5 μm in diameter) were trapped with the same laser power at different perpendicular positions. There was an increase in particle displacement at 2 μm or less from the glass surface that implied a viscous coupling to the coverslip surface. From 2 μm to 5 μm above the surface, the force on the beads in the trap was constant. This calibration was used to calculate the forces that form tethers. All these experiments were performed 3–4 μm above the coverslip surface to minimized viscous coupling to the glass surface, and the laser power was simultaneously monitored.

Laser Tweezers Manipulations

To prepare samples for observation, the cloning cylinder was removed, and the coverslip containing the cells was mounted on an aluminum coverslip holder with silicone grease; then a second cleaned coverslip was mounted on top to form a flow cell. The IgG-covered latex beads and anti-FL antibody-coated bead suspensions in medium were exchanged for the normal medium. The growth cones were viewed by a video-enhanced differential interference contrast (DIC) microscope (IM-35 microscope; Zeiss, Oberkochen, Germany) with a fiber optic illuminator. The stage was maintained at 38°C by using an air current incubator. The laser trap consisted of a polarized beam from an 11 W TEM00-mode near-infrared (1064 nm) Nd:YAG laser (model 116Fn, Quantronix Corp., Smithtown, NY) that was expanded by a 3× beam expander (Newport Corporation, Irvine, CA), then focused through an 80 mm focal length achromatic lens (Melles Griot, Irvine, CA) into the epifluorescence port of a Zeiss IM-35 microscope (Kuo and Sheetz, 1992). To measure axon extension, the nerve growth cone positions were recorded on video tape and analyzed later by a ruler program. To observe the diffusing bead movements on the axons, beads were held at the axon surface by the laser optical tweezers with ~40 mW of power. To label cells with FL-PE, the DRG cells were first incubated with 1 μg/ml FL-PE (Molecular Probes, Eugene, OR) in the medium for 15 min before exchange with fresh medium. Videotape records of the diffusing beads were analyzed off-line. For the experiments in which flow was created by tether formation, two or three IgG- or anti-FL-coated beads were placed on the axon with the laser optical tweezers. The central bead was used to form a tether of 15 μm in length with the laser tweezers (60 mW of laser power). Positions of the other bead(s) were recorded before and immediately after tether formation, and the displacement caused by tether formation was determined.

To measure the membrane static tether force at different regions along the axon, IgG-coated beads were bound to the axon near the cell body or near the growth cone (approximately 4 μm into the axon). Then the bead was pulled out at a constant velocity and held for several seconds at a constant tether length (~15 μm). To measure the static tether force, F_S, the position of the bead in the trap during the stationary phase was measured with the nanometer-scale tracking program that had been developed previously (Gelles et al., 1988), and the force (F) of the tether on the bead was calculated from the calibration of the laser trap.

Acknowledgments

Correspondence should be addressed to M. P. S. We thank our colleagues Z. Wang and R. Sterba for their kind help in part of this work. We also thank members of the Sheetz laboratory for their helpful discussion about this work, and Drs. T. Meyer and G. Banker for their helpful comments on this manuscript. This work was supported by grants from the National Institutes of Health, the Human Frontier Science Project, and the Muscular Dystrophy Association.

Received September 5, 1995; revised October 3, 1995.

References

Berk, D.A., and Hochmuth, R.M. (1992). Lateral mobility of integral proteins in red blood cell tethers. Biophys. J. *61*, 9–18.

Bray, D. (1970). Surface movements during the growth of single explanted neurons. Proc. Natl. Acad. Sci. USA *65*, 905–910.

Bretscher, M.S. (1984). Endocytosis: relation to capping and cell locomotion. Science *224*, 681–686.

Craig, A.M., Wyborski, R.J., and Banker, G. (1995). Preferential addition of newly synthesized membrane protein at axonal growth cones. Nature *375*, 592–594.

Dai, J., and Sheetz, M.P. (1995a). Mechanical properties of neuronal growth cone membranes studied by tether formation with laser optical

tweezers. Biophys. J. *68*, 988–996.

Dai, J., and Sheetz, M.P. (1995b). Regulation of endocytosis, exocytosis and shape by membrane tension. Cold Spring Harbor Symp. Quant. Biol. *60*, in press.

Debrabander, M., Nuydens, R., Ishihara, A., Holifield, B., Jacobson, K., and Geerts, H. (1991). Lateral diffusion and retrograde movements of individual cell surface components on single motile cells observed with nanovid microscopy. J. Cell Biol. *112*, 111–124.

Edidin, M., Kuo, S., and Sheetz, M.P. (1991). Lateral movements of membrane glycoproteins restricted by dynamic cytoplasmic barriers. Science *254*, 1379–1382.

Gelles, J., Schnapp, B.J., and Sheetz, M.P. (1988). Tracking kinesin-driven movements with nanometer-scale precision. Nature *331*, 450–453.

Griffin, J.W., Price, D.L., Drachman, D.B., and Morris, J. (1981). Incorporation of axolemma during nerve regeneration. J. Cell Biol. *88*, 205–214.

Heidemann, S.R., Lamoureux, P., and Buxbaum, R.E. (1990). Growth cone behavior and production of traction force. J. Cell Biol. *111*, 1949–1957.

Hochmuth, R.M., Shao, J., Dai, J., and Sheetz, M.P. (1995). Deformation and flow of membrane into tethers extracted from neuronal growth cones. Biophys. J., in press.

Ishihara, A., and Jacobson, K. (1993). A closer look at how membrane proteins move. Biophys. J. *65*, 1754–1756.

Kucik, D.F., Elson, E.L., and Sheetz, M.P. (1990). Cell migration does not produce membrane flow. J. Cell Biol. *111*, 1617–1622.

Kuo, S.C., and Sheetz, M.P. (1993). Force of single kinesin molecules measured with optical tweezers. Science *260*, 232–234.

Kuo, S.C., and Sheetz, M.P. (1992). Optical tweezers in cell biology. Trends Cell Biol. *2*, 116–118.

Lee, G.M., Ishihara, A., and Jacobson, K.A. (1991). Direct observation of Brownian motion of lipids in a membrane. Proc. Natl. Acad. Sci. USA *88*, 6274–6278.

Lee, G.M., Ishihara, A., Theriot, J.A., and Jacobson, K.A. (1993). Principles of locomotion for simple-shaped cells. Nature *362*, 167–171.

Lee, J., Gustafsson, M., Magnusson, K., and Jacobson, K. (1990). The direction of membrane lipid flow in locomoting polymorphonuclear leukocytes. Science *247*, 1229–1233.

Martenson, C., Stone, K., Reedy, M., and Sheetz, M. (1993). Fast axonal transport is required for growth cone advance. Nature *366*, 66–69.

Okabe, S., and Hirokawa, N. (1990). Turnover of fluorescently labeled tubulin and actin in the axon. Nature *343*, 479–482.

Okabe, S., and Hirokawa, N. (1993). Do photobleached fluorescent microtubules move? Re-evaluation of fluorescence laser photobleaching both in vitro and in growing *Xenopus* axons. J. Cell Biol. *120*, 1177–1186.

Pfenninger, K.H., and Maylie-Pfenninger, M.-F. (1981). Lectin labeling of sprouting neurons. II. Relative movement and appearance of glycoconjugates during plasmalemmal expansion. J. Cell Biol. *89*, 547–559.

Popov, S., Brown, A., and Poo, M. (1993). Forward plasma membrane flow in growing nerve processes. Science *259*, 244–246.

Reinsch, S.S., Mitchison, T.J., and Kirschner, M. (1991). Microtubule polymer assembly and transport during axonal elongation. J. Cell Biol. *115*, 365–379.

Qian, H., Sheetz, M.P., and Elson, E.L. (1991). Single particle tracking: analysis of diffusion and flow in two-dimensional systems. Biophys. J. *60*, 910–921.

Schnapp, B.J., Gelles, J., and Sheetz, M.P. (1988). Nanometer-scale measurements using video light microscopy. Cell Motil. Cytoskel. *10*, 47–53.

Sheetz, M.P., Turney, S., Qian, H., and Elson, E.L. (1989). Nanometre-level analysis demonstrates that lipid flow does not drive membrane glycoprotein movements. Nature *340*, 284–288.

Sheetz, M.P., Baumrind, N.L., Wayne, D.S., and Pearlman, A.L. (1990). Concentration of membrane antigens by forward transport and trapping in neuronal growth cones. Cell *61*, 231–241.

Smith, R.S., Hammerschlag, R., Snyder, R.E., Chan, H., and Bobinski, J. (1994). Action of brefeldin A on amphibian neurons: passage of newly synthesized proteins through the Golgi complex is not required for continued fast organelle transport in axons. J. Neurochem. *62*, 1698–1706.

Steinman, R.M., Mellman, I.S., Muller, W.A., Cohn, Z.A. (1983). Endocytosis and the recycling of plasma membrane. J. Cell Biol. *96*, 1–27.

Svoboda, K., Schmidt, C.F., Schnapp, B.J., and Block, S.M. (1993). Direct observation of kinesin stepping by optical trapping interferometry. Nature *365*, 721–727.

Vance, J.E., Pan, D., Vance, D.E., and Campenot, R.B. (1991). Biosynthesis of membrane lipids in rat axons. J. Cell Biol. *115*, 1061–1068.

Waugh, R.E., and Hochmuth, R.M. (1987). Mechanical equilibrium of thick, hollow, liquid membrane cylinders. Biophys. J. *52*, 391–400.